2024 32nd Mediterranean Conference on Control and Automation (MED)
June 11-14, 2024 | Chania, Crete, Greece

Safe MPC-based Motion Planning of AUVs Using MHE-based Approximate Robust Control Barrier Functions

Hossein Nejatbakhsh Esfahani and Javad Mohammadpour Velni

Abstract— **This paper presents a safety-critical motion planning approach for Autonomous Underwater Vehicles (AUVs). To this end, we formulate a safe Model Predictive Control (MPC) scheme by leveraging the benefits of MPC with a discrete-time Control Barrier Function (CBF). To address the truncation errors associated with the discretized CBF, we then adopt a Moving Horizon Estimation (MHE) approach to approximate these errors. To cope with both the model mismatch in the CBF and unknown external disturbances, we also leverage the MHE scheme to formulate an approximate Robust CBF (RCBF). Finally, to demonstrate the efficacy of the proposed safety-critical robust control scheme, simulation studies are conducted for path planning of AUVs, and the results confirm the superiority of the proposed method compared to few other methods.**

I. Introduction

Autonomous Underwater Vehicles (AUVs) have been employed for various missions such as non-invasive testing of marine structures or underwater oil/gas pipelines, as well as ocean exploration [1], to name a few. Motion planning is an important task in AUV navigation that is critical in finding a collision-free and feasible path from the initial position to the target position under certain evaluation criteria such as optimal path length or minimum energy consumption.

The recent enhancements in computational power and optimization techniques have provided an opportunity for Model Predictive Control (MPC) to be used in the maritime applications with limited onboard computational resources. MPC is a popular and widely used approach for the optimal control design. This optimization-based control approach is often selected due to its capability to handle both input and state constraints [2]. The MPC-based motion planning offers significant benefits for the safer operations of constrained AUVs in complex environments. Previous studies have explored the inclusion of safety considerations within MPC framework to ensure that the controlled system operates within predefined safety boundaries. For example, barrier functions were utilized to develop a safety-critical MPC with Control Barrier Functions (CBFs) in [3], [4].

Using CBFs has become popular for synthesizing safety-critical controllers due to their generality and relative ease of synthesis and implementation [5]. Barrier functions made their debut in optimization theory and, and now they are frequently mentioned in control and verification literature because of their bond with Lyapunov-like functions, their ability to establish safety and avoidance, and their association with multi-objective control [6], [7]. Although CBF is a popular tool to achieve provable safety guarantees, designing CBFs and calculating the corresponding safe control inputs may be nontrivial in the presence of external disturbances. Safety criteria within the scope of MPC are commonly expressed as constraints of the underlying optimization problem, as demonstrated in previous works [8], [3]. These constraints encompass factors such as obstacles and actuation limits. An example of a specific situation where safety criteria are relevant in robotics is obstacle avoidance [9]. However, they only restrict the movement of a robot when it is in close proximity of obstacles. In order to prompt the robot to take preventive actions even when obstacles are far away, a larger prediction horizon is typically required. Nevertheless, this elongated horizon leads to increased computational time during the optimization process. As a result, there is a motivation to develop a novel form of predictive controls that ensures safety within the framework of set invariance. This approach employs the CBF constraints to confine the robot's movement throughout the optimization process [6].

Although CBF-based control design approaches have emerged as highly effective safety-critical control tools, the effectiveness of CBFs heavily relies on the precision and fidelity of the model employed for making the CBF constraints. To cope with external disturbances in the CBF-based control design, robust CBF schemes have been recently proposed [10], [11]. However, proposed robust CBFs in the literature are formulated in the continuous-time domain while the control implementation is done in discrete time. To allow using the continuous-time safety analysis and design a discrete-time robust CBF in the context of CBF-MPC, in this work, we propose to tackle the truncation errors due to the discretization of the continuous-time CBFs using a Moving Horizon Estimation (MHE) scheme. MHE is an optimization-based estimator/observer and a simple choice that, combined with an MPC scheme, works on a horizon window covering a limited history of past measurements [12]. Moreover, we leverage the MHE scheme to formulate an approximate robust CBF (RCBF) in order to cope with both model mismatch in the CBF and unknown external disturbances.

The paper is structured as follows. A dynamic model of AUVs used in this work is described in Section II. Section III provides background information on the control barrier functions. The proposed approximate RCBF is detailed in Section IV. In Section V, a safe MPC-based motion planning method is presented, which is formulated using the proposed MHE-based RCBF. The simulation results and discussions

*This work was supported by the US National Science Foundation under award #2302217.

Authors are with the Department of Mechanical Engineering, Clemson University, Clemson, SC, USA. {hnejatb, javadm}@clemson.edu.

are given in Section VI. Finally, concluding remarks are made in Section VII.

II. Description of the AUV Dynamic Model

To provide a dynamic model of an AUV, one can assume that the pitch and roll motions are intrinsically stable due to the effect of the buoyancy force. However, we assume that there is a higher level controller as autopilot to track the desired roll and pitch angles. Therefore, the 6-DOF platform can be reduced to the fully actuated 4-DOF model with the following nonlinear equations [13]:

$$\dot{\boldsymbol{\eta}} = J(\boldsymbol{\eta})\boldsymbol{v}, \tag{1a}$$

$$M\dot{\boldsymbol{v}} + C(\boldsymbol{v})\boldsymbol{v} + D(\boldsymbol{v})\boldsymbol{v} + \mathrm{g}(\boldsymbol{\eta}) = \boldsymbol{\tau} + \boldsymbol{\tau}_d \tag{1b}$$

where $\boldsymbol{\eta} = [x, y, z, \psi]^\top$ is the position-orientation (yaw angle) vector, and $\boldsymbol{v} = [u, v, w, r]^\top$ denotes the velocity vector for the surge, sway, heave and yaw motions, respectively. Furthermore, $M, C(\boldsymbol{v}), D(\boldsymbol{v}) \in \mathbb{R}^{4\times4}$ are the inertia matrix (including the effects of added mass), Coriolis-centripetal matrix and the drag force matrix (hydrodynamic damping), respectively. The vector of forces and moments induced by the gravity and buoyancy is labeled by $\mathrm{g} \in \mathbb{R}^{4\times1}$. The control inputs and the external time-varying disturbances (winds, waves, and ocean currents) are labeled as $\boldsymbol{\tau}, \boldsymbol{\tau}_d \in \mathbb{R}^{4\times1}$, respectively. The transformation matrix between the reference frames can be represented in Euler angles as

$$J(\boldsymbol{\eta}) = \begin{bmatrix} \cos(\psi) & -\sin(\psi) & 0 & 0 \\ \sin(\psi) & \cos(\psi) & 0 & 0 \\ 0 & 0 & 1 & 0 \\ 0 & 0 & 0 & 1 \end{bmatrix}. \tag{2}$$

Let $M = \mathrm{diag}\{m_{11}, m_{22}, m_{33}, m_{44}\}$ be the inertia matrix. Then, the diagonal terms are $m_{11} = m - X_{\dot{u}}$, $m_{22} = m - Y_{\dot{v}}$, $m_{33} = m - Z_{\dot{w}}$, $m_{44} = I_z - N_{\dot{r}}$, where m is the total mass of AUV and I_z is the moment of inertia about the yaw motion. The corresponding hydrodynamic coefficients are labeled by $X_\star$, $Y_\star$, $Z_\star$, $N_\star$. Then, the Coriolis–centripetal matrix is expressed as

$$C(\boldsymbol{v}) = \begin{bmatrix} 0 & 0 & 0 & -(m - Y_{\dot{v}})v \\ 0 & 0 & 0 & (m - X_{\dot{u}})u \\ 0 & 0 & 0 & 0 \\ (m - Y_{\dot{v}})v & -(m - X_{\dot{u}})u & 0 & 0 \end{bmatrix}. \tag{3}$$

Let $D(\boldsymbol{v}) = \mathrm{diag}\{d_{11}, d_{22}, d_{33}, d_{44}\}$ be the damping matrix. Then, the diagonal terms are $d_{11} = -X_u - X_{|u|u}|u|$, $d_{22} = -Y_v - Y_{|v|v}|v|$, $d_{33} = -Z_w - Z_{|w|w}|w|$, and $d_{44} = -N_r - N_{|r|r}|r|$. The gravity-buoyancy vector is

$$\mathrm{g} = [0, 0, -(G - B), 0]^\top, \tag{4}$$

where G and B are the gravity and buoyancy forces, respectively. Then, one can rewrite (1) as

$$M(\boldsymbol{\eta})\ddot{\boldsymbol{\eta}} + C(\dot{\boldsymbol{\eta}}, \boldsymbol{\eta})\dot{\boldsymbol{\eta}} + D(\dot{\boldsymbol{\eta}}, \boldsymbol{\eta})\dot{\boldsymbol{\eta}} + \mathrm{g}(\boldsymbol{\eta}) = \bar{\boldsymbol{\tau}} + \bar{\boldsymbol{\tau}}_d, \tag{5}$$

where

$$M(\boldsymbol{\eta}) = J^{-T} M J^{-1}(\boldsymbol{\eta}), \tag{6a}$$

$$C(\dot{\boldsymbol{\eta}}, \boldsymbol{\eta}) = J^{-T}\left[C(\boldsymbol{v}) - MJ^{-1}(\boldsymbol{\eta})\dot{J}(\boldsymbol{\eta})\right] J^{-1}(\boldsymbol{\eta}), \tag{6b}$$

$$D(\dot{\boldsymbol{\eta}}, \boldsymbol{\eta}) = J^{-T} D(\boldsymbol{v}) J^{-1}(\boldsymbol{\eta}), \tag{6c}$$

$$\bar{\boldsymbol{\tau}} = J^{-T}\boldsymbol{\tau}, \tag{6d}$$

$$\bar{\boldsymbol{\tau}}_d = J^{-T}\boldsymbol{\tau}_d. \tag{6e}$$

In practice, the aforementioned system dynamics includes uncertain parameters. Let $\Delta M, \Delta C, \Delta D, \Delta \mathrm{g}$ be the uncertain parts of each parameter matrix or vector. Then, the entire model of AUV can be rewritten as

$$M(\boldsymbol{\eta})\ddot{\boldsymbol{\eta}} + C(\dot{\boldsymbol{\eta}}, \boldsymbol{\eta})\dot{\boldsymbol{\eta}} + D(\dot{\boldsymbol{\eta}}, \boldsymbol{\eta})\dot{\boldsymbol{\eta}} + \mathrm{g}(\boldsymbol{\eta}) = \bar{\boldsymbol{\tau}} + \boldsymbol{p}, \tag{7}$$

where the perturbation $\boldsymbol{p}$ includes the external time-varying disturbances $\boldsymbol{\tau}_d$ and model uncertainties δ as

$$\begin{aligned} \boldsymbol{p} =& \bar{\boldsymbol{\tau}}_d - J^{-T}\Delta M J^{-1}(\boldsymbol{\eta})\ddot{\boldsymbol{\eta}} \\ & - J^{-T}\left[\Delta C(\boldsymbol{v}) - \Delta M J^{-1}(\boldsymbol{\eta})\dot{J}(\boldsymbol{\eta})\right] J^{-1}(\boldsymbol{\eta})\dot{\boldsymbol{\eta}} \\ & - J^{-T}\Delta D(\boldsymbol{v}) J^{-1}(\boldsymbol{\eta}) - \Delta \mathrm{g}(\boldsymbol{\eta}) = \bar{\boldsymbol{\tau}}_d - \delta. \end{aligned} \tag{8}$$

Let us now define $\boldsymbol{x}_1 = \boldsymbol{\eta}$ and $\boldsymbol{x}_2 = \dot{\boldsymbol{\eta}}$ as state variables, and so the concatenated state vector is $\boldsymbol{x} = [\boldsymbol{x}_1, \boldsymbol{x}_2]^\top$. Then, the system (7) can be described in control-affine form as

$$\begin{aligned} \dot{\boldsymbol{x}} &= \boldsymbol{f}(\boldsymbol{x}) + g(\boldsymbol{x})\boldsymbol{\tau} + \tilde{\boldsymbol{f}}(\boldsymbol{x}) \\ \boldsymbol{y} &= \boldsymbol{x}_1 \end{aligned} \tag{9}$$

where $\boldsymbol{f} = \left[\boldsymbol{x}_2, \bar{\boldsymbol{f}}\right]^\top$, $g = [0_{4\times4}, \bar{g}]^\top$, $\tilde{\boldsymbol{f}}(\boldsymbol{x}) = [0_{4\times1}, \boldsymbol{d}(\boldsymbol{x}_1)]^\top$ and

$$\bar{\boldsymbol{f}}(\boldsymbol{x}) = M^{-1}(\boldsymbol{x}_1)\Big(- C(\boldsymbol{x}_1, \boldsymbol{x}_2)\boldsymbol{x}_2 - D(\boldsymbol{x}_1, \boldsymbol{x}_2)\boldsymbol{x}_2 - \mathrm{g}\Big), \tag{10a}$$

$$\bar{g} = M^{-1}(\boldsymbol{x}_1)J^{-T}, \tag{10b}$$

$$\boldsymbol{d}(\boldsymbol{x}_1) = M^{-1}(\boldsymbol{x}_1)\boldsymbol{p}. \tag{10c}$$

III. Review of Control Barrier Functions

In the context of safety-critical systems, the control barrier functions (CBFs) are adopted to provide an admissible control input space for safety assurance of dynamical systems. More specifically, safety can be formulated in the context of enforcing invariance of a set, i.e., not leaving a safe set.

A. Continuous-Time CBFs

Let us consider a set $\mathcal{C}$ defined as the super-level set of a continuously differentiable function $h : \mathcal{D} \subset \mathbb{R}^n \to \mathbb{R}$ such that

$$\begin{aligned} \mathcal{C} &= \{\boldsymbol{x} \in \mathcal{D} \subset \mathbb{R}^n : h(\boldsymbol{x}) \geq 0\}, \\ \partial\mathcal{C} &= \{\boldsymbol{x} \in \mathcal{D} \subset \mathbb{R}^n : h(\boldsymbol{x}) = 0\}, \\ \mathrm{Int}(\mathcal{C}) &= \{\boldsymbol{x} \in \mathcal{D} \subset \mathbb{R}^n : h(\boldsymbol{x}) > 0\}, \end{aligned} \tag{11}$$

where $\partial\mathcal{C}$ and $\mathrm{Int}(\mathcal{C})$ are the boundary of $\mathcal{C}$ and the interior of $\mathcal{C}$, respectively. We additionally assume that $\mathrm{Int}(\mathcal{C}) \neq \emptyset$. We then refer to $\mathcal{C}$ as the *safe set* so that a CBF certifies whether a control policy achieves forward invariance of $\mathcal{C}$ by evaluating if the system trajectory remains away from

the boundary of $\mathcal{C}$. Let us consider a nonlinear system in control-affine form as

$$\dot{\boldsymbol{x}} = \boldsymbol{f}(\boldsymbol{x}) + g(x)\,\boldsymbol{u}, \tag{12}$$

where $f : \mathbb{R}^n \to \mathbb{R}^n$ and $g : \mathbb{R}^n \to \mathbb{R}^{n\times m}$ are locally Lipschitz continuous functions, $\boldsymbol{x} \in \mathbb{R}^n$ and $\boldsymbol{u} \in \mathbb{R}^m$ are the system states and control inputs. The closed-loop dynamics then is

$$\dot{\boldsymbol{x}} = \boldsymbol{f}_{\text{cl}}(\boldsymbol{x}) = \boldsymbol{f}(\boldsymbol{x}) + g(x)\,\boldsymbol{u}|_{\boldsymbol{\pi}(\boldsymbol{x})}, \tag{13}$$

where the control policy (feedback controller) $\boldsymbol{\pi} : \mathbb{R}^n \to \mathbb{R}^m$ is locally Lipschitz continuous. Then, one can consider a maximum interval of existence $I(\boldsymbol{x}_0) = [t_0, t_{\max})$ for any initial condition $\boldsymbol{x}_0 \in \mathcal{D}$ such that $\boldsymbol{x}(t)$ is the unique solution to (13) on $I(\boldsymbol{x}_0)$. In the case $t_{\max} = \infty$, the closed-loop system $\boldsymbol{f}_{\text{cl}}$ is forward complete.

Definition 1. *[6] (Forward Invariant) The closed-loop system* (13) *is forward invariant w.r.t the set $\mathcal{C}$ if for every $\boldsymbol{x}_0 \in \mathcal{C}$, we have $\boldsymbol{x}(t) \in \mathcal{C}$ for all $t \in I(\boldsymbol{x}_0)$.*

Definition 2. *[6] (Control Barrier Function) Given a dynamic system described by* (12) *and the safe set $\mathcal{C}$ with a continuously differentiable function $h : \mathcal{D} \to \mathbb{R}$, then h is a CBF if there exists a class $\mathcal{K}_\infty$ function κ for all $\boldsymbol{x} \in \mathcal{D}$ such that*

$$\sup_{\boldsymbol{u}\in\mathcal{U}} \left\{ \underbrace{\nabla h(\boldsymbol{x})^\top \left(\boldsymbol{f}(\boldsymbol{x}) + g(\boldsymbol{x})\,\boldsymbol{u}\right)}_{\dot{h}(\boldsymbol{x},\boldsymbol{u})} \right\} \geq -\kappa\left(h(\boldsymbol{x})\right). \tag{14}$$

The affine CBF condition then reads as

$$\text{CBF}(\boldsymbol{x},\boldsymbol{u}) = \nabla h(\boldsymbol{x})^\top \left(\boldsymbol{f}(\boldsymbol{x}) + g(\boldsymbol{x})\,\boldsymbol{u}\right) + \kappa\left(h(\boldsymbol{x})\right) \geq 0. \tag{15}$$

However, the affine CBF above assumes the control signal $\boldsymbol{u}$ is applied to the real system in continuous-time, while in practice, controllers generate discrete-time signals.

B. Discrete-time CBFs

In this paper, we consider a nonlinear MPC scheme to control an AUV, where the discrete-time control input signals delivered from the MPC scheme are defined as

$$\boldsymbol{u}(\tau) = \boldsymbol{u}_k, \quad \forall \tau \in [t_k, t_{k+1}), \tag{16}$$

where $\boldsymbol{u}_k \in \mathcal{U}$ is computed at time instant t_k and applied over the interval $[t_k, t_{k+1})$ with the sampling time of $T = t_{k+1} - t_k$. To use a CBF in the MPC scheme, a discrete-time CBF can be formulated as [3]

$$\Delta h(\boldsymbol{x}_k, \boldsymbol{u}_k) \geq -\gamma h(\boldsymbol{x}_k), \quad 0 < \gamma \leq 1. \tag{17}$$

However, the discrete-time CBF condition (17) may not hold in the presence of uncertainties, disturbances and imperfect safety function h. Moreover, it is not straightforward to modify the condition above in order to capture a robust discrete-time CBF, whereas the safety and robustness analysis can be readily guaranteed in continuous time upon the CBF condition (14) [14]. To address this issue and formulate a discrete-time controller, e.g., an MPC scheme with continuous-time safety guarantees, a discrete-time version of the CBF condition (15) can be formulated as [15]

$$\text{CBF}(\boldsymbol{x}_\tau, \boldsymbol{u}_k) \geq 0, \tag{18a}$$

$$\text{CBF}(\boldsymbol{x}_\tau, \boldsymbol{u}_k) = \nabla h(\boldsymbol{x}_\tau)^\top \left(\boldsymbol{f}(\boldsymbol{x}_\tau) + g(\boldsymbol{x}_\tau)\,\boldsymbol{u}_k\right) + \kappa\left(h(\boldsymbol{x}_\tau)\right), \tag{18b}$$

where

$$\boldsymbol{f}(\boldsymbol{x}_\tau) = \boldsymbol{f}(\boldsymbol{x}_k) + \boldsymbol{w}_f, \tag{19a}$$

$$g(\boldsymbol{x}_\tau) = g(\boldsymbol{x}_k) + w_g, \tag{19b}$$

$$h(\boldsymbol{x}_\tau) = h(\boldsymbol{x}_k) + w_h, \tag{19c}$$

$$\nabla h(\boldsymbol{x}_\tau) = \nabla h(\boldsymbol{x}_k) + \boldsymbol{w}_{\nabla h}, \tag{19d}$$

and the set of possible disturbances $\boldsymbol{w}_d = \{\boldsymbol{w}_f, w_g, w_h, \boldsymbol{w}_{\nabla h}\}$ includes the truncation errors due to the discretization. A tube-based CBF was proposed in [15] to robustify the discrete-time CBF condition (18) against the truncation errors. However, designing an accurate tube to provide an adequate robustness against the truncation errors and additional disturbances/model uncertainties is challenging in particular for the large-scale nonlinear systems with unknown disturbances. To address this issue and design an approximate robust discrete-time CBF for AUVs, we then propose to approximate the augmented disturbances using an MHE scheme detailed in the next section.

IV. Approximate Robust CBF

Let us define combined disturbances $\bar{\boldsymbol{w}}_d$, including both the truncation error and model uncertainty/disturbance, as

$$\bar{\boldsymbol{w}}_d = \left\{ \underbrace{\boldsymbol{w}_f + \tilde{\boldsymbol{f}}}_{\bar{\boldsymbol{w}}_f}, w_g, \underbrace{w_h + \tilde{h}}_{\bar{w}_h}, \underbrace{\boldsymbol{w}_{\nabla h} + \nabla\tilde{h}}_{\bar{\boldsymbol{w}}_{\nabla h}} \right\}, \tag{20}$$

where $\tilde{\boldsymbol{f}}, \tilde{h}, \nabla\tilde{h}$ are unknown disturbances. Assume that we do not have access to an accurate model of the real (true) safety function h, and let h_a be an approximation model (an imperfect model) of the real safety function h. We then have that $\bar{w}_h(\boldsymbol{x}) = h(\boldsymbol{x}) - h_a(\boldsymbol{x})$ and $\bar{\boldsymbol{w}}_{\nabla h}(\boldsymbol{x}) = \nabla h(\boldsymbol{x}) - \nabla h_a(\boldsymbol{x})$.

Assumption 1. *The unknown errors are uniformly bounded such that*

$$|\bar{w}_h(\boldsymbol{x})| \leq e_h(\boldsymbol{x}), \quad |\bar{\boldsymbol{w}}_{\nabla h}(\boldsymbol{x})| \leq e_{\nabla h}(\boldsymbol{x}) \tag{21}$$

for some $e_h(\boldsymbol{x}) : \mathbb{R}^n \to \mathbb{R}_{\geq 0}$ and $e_{\nabla h}(\boldsymbol{x}) : \mathbb{R}^n \to \mathbb{R}_{\geq 0}$.

Assumption 2. *There exists an observer, e.g., an MHE scheme, to estimate $\boldsymbol{w}_f, w_g, \tilde{\boldsymbol{f}}, e_{\nabla h}, e_h$.*

Note that the bounds $e_{\nabla h}, e_h$ can be directly obtained from an exact safety function h. However, we additionally assume that these bounds are unknown.

Theorem 1. *Under Assumptions 1, 2 and considering a linear form of $\kappa(h(\boldsymbol{x}_\tau)) = \alpha h(\boldsymbol{x}_\tau)$, a discrete-time CBF is then*

an approximate robust CBF (RCBF) using an imperfect safety function h_a such that

$$\begin{aligned}(\nabla h_a(\boldsymbol{x}_k))^\top \Big(\boldsymbol{f}(\boldsymbol{x}_k)+\bar{\boldsymbol{w}}_f+(g(\boldsymbol{x}_k)+w_g)\boldsymbol{u}_k\Big) \\ +\alpha(h_a(\boldsymbol{x}_k)-e_h(\boldsymbol{x}_k)) \\ \geq \|\boldsymbol{f}(\boldsymbol{x}_k)+\bar{\boldsymbol{w}}_f+(g(\boldsymbol{x}_k)+w_g)\boldsymbol{u}_k\|\, e_{\nabla h}(\boldsymbol{x}_k)\end{aligned} \tag{22}$$

and $\boldsymbol{u}_k$ guarantees that the safe set $\mathcal{C}$ is forward invariant.

Proof. Considering the combined disturbances (20) and substituting (19) in (18), the discrete-time CBF condition then reads as

$$\begin{aligned}(\nabla h_a(\boldsymbol{x}_k))^\top(\boldsymbol{f}(\boldsymbol{x}_k)+\bar{\boldsymbol{w}}_f+(g(\boldsymbol{x}_k)+w_g)\boldsymbol{u}_k) \\ +(\bar{\boldsymbol{w}}_{\nabla h}(\boldsymbol{x}_k))^\top(\boldsymbol{f}(\boldsymbol{x}_k)+\bar{\boldsymbol{w}}_f+(g(\boldsymbol{x}_k)+w_g)\boldsymbol{u}_k) \\ \geq -\kappa(h_a(\boldsymbol{x}_k)+\bar{w}_h).\end{aligned} \tag{23}$$

To robustify the condition above, the minimum value of the left-hand side in the inequality (23) must be greater than the maximum value of the right-hand side for any $\boldsymbol{x}_k$, and any $\bar{w}_h(\boldsymbol{x}_k)$ and $\bar{\boldsymbol{w}}_{\nabla h}(\boldsymbol{x}_k)$ satisfying (21) in order to ensure that (18) still holds. We then have that

$$\begin{aligned}\min_{|\bar{\boldsymbol{w}}_{\nabla h}(\boldsymbol{x}_k)|\leq e_{\nabla h}(\boldsymbol{x}_k)} (\nabla h_a(\boldsymbol{x}_k))^\top\Big(\boldsymbol{f}(\boldsymbol{x}_k)+\bar{\boldsymbol{w}}_f \\ +(g(\boldsymbol{x}_k)+w_g)\boldsymbol{u}_k\Big) \\ +(\bar{\boldsymbol{w}}_{\nabla h}(\boldsymbol{x}_k))^\top(\boldsymbol{f}(\boldsymbol{x}_k)+\bar{\boldsymbol{w}}_f+(g(\boldsymbol{x}_k)+w_g)\boldsymbol{u}_k) \\ \geq \max_{|\bar{w}_h(\boldsymbol{x}_k)|\leq e_h(\boldsymbol{x}_k)} -\kappa(h_a(\boldsymbol{x}_k)+\bar{w}_h(\boldsymbol{x}_k))\end{aligned} \tag{24}$$

The minimum value of the left-hand side is then obtained when $\bar{\boldsymbol{w}}_{\nabla h}(\boldsymbol{x}_k)$ is in the opposite direction to the gradient of $(\boldsymbol{f}(\boldsymbol{x}_k)+\bar{\boldsymbol{w}}_f+(g(\boldsymbol{x}_k)+w_g)\boldsymbol{u}_k)$. Since κ is an extended class $\mathcal{K}$ function and $e_h(\boldsymbol{x}_k)\geq 0$, the maximum value of the right-hand side then reads as $-\kappa(h_a(\boldsymbol{x}_k)-e_h(\boldsymbol{x}_k))$. The approximate robust discrete-time CBF condition is then expressed as

$$\begin{aligned}(\nabla h_a(\boldsymbol{x}_k))^\top(\boldsymbol{f}(\boldsymbol{x}_k)+\bar{\boldsymbol{w}}_f+(g(\boldsymbol{x}_k)+w_g)\boldsymbol{u}_k) \\ +\kappa(h_a(\boldsymbol{x}_k)-e_h(\boldsymbol{x}_k)) \\ \geq \|\boldsymbol{f}(\boldsymbol{x}_k)+\bar{\boldsymbol{w}}_f+(g(\boldsymbol{x}_k)+\bar{w}_g)\boldsymbol{u}_k\|\, e_{\nabla h}(\boldsymbol{x}_k).\end{aligned} \tag{25}$$

We then have that

$$\kappa(h_a(\boldsymbol{x}_k)-e_h(\boldsymbol{x}_k))=\alpha(h_a(\boldsymbol{x}_k)-e_h(\boldsymbol{x}_k)). \tag{26}$$

By substituting (26) in (25), the condition (22) is then obtained. ■

In the present paper, we propose a linear combination of candidate CBFs. Moreover, we use this parametric CBF in the context of MPC, where the mapping function κ in (26) is constructed as a polynomial function containing independent odd-powered safety functions $h_a(\boldsymbol{x}_k)$, which are candidate class $\mathcal{K}$ functions [16]. This parametric CBF can regulate how fast the state of the system can approach the boundary of the safe set $\mathcal{C}$. The approximate RCBF condition (22) then reads as

$$\begin{aligned}(\nabla h_a(\boldsymbol{x}_k))^\top\Big(\boldsymbol{f}(\boldsymbol{x}_k)+\bar{\boldsymbol{w}}_f+(g(\boldsymbol{x}_k)+w_g)\boldsymbol{u}_k\Big) \\ +(\boldsymbol{H}(\boldsymbol{x}_k)-\boldsymbol{e}_h(\boldsymbol{x}_k))^\top\boldsymbol{\alpha} \\ \geq \|\boldsymbol{f}(\boldsymbol{x}_k)+\bar{\boldsymbol{w}}_f+(g(\boldsymbol{x}_k)+w_g)\boldsymbol{u}_k\|\, e_{\nabla h}(\boldsymbol{x}_k),\end{aligned} \tag{27}$$

where (for $p\in\mathcal{N}$)

$$\boldsymbol{H}(\boldsymbol{x}_k)=\Big[h_a(\boldsymbol{x}_k),(h_a(\boldsymbol{x}_k))^3,\ldots,(h_a(\boldsymbol{x}_k))^{2p-1}\Big]^\top. \tag{28}$$

To provide an adaptive structure for the parametric CBFs, we then use MHE scheme to estimate the parameters associated with the proposed approximate RCBF condition (27).

V. Safe MPC-based Motion Planning

In this section, we formulate the safety-critical MPC problem using the proposed approximate RCBF (27), where the parameters $\hat{\boldsymbol{d}}=\{\bar{\boldsymbol{w}}_f,w_g,\boldsymbol{e}_h^n,e_{\nabla h}^n\},n=1,\ldots,n_{\text{cbf}}$ are estimated by the following MHE scheme

$$\begin{aligned}&\Big\{\hat{\boldsymbol{d}}_k,\hat{\boldsymbol{x}}_{k-N_{\text{MHE}},\ldots,k},\hat{\boldsymbol{u}}_{k-N_{\text{MHE}},\ldots,k-1}\Big\} \\ &\quad=\underset{\boldsymbol{x},\boldsymbol{u},\boldsymbol{d}}{\arg\min}\,\|\boldsymbol{x}_{k-N_{\text{MHE}}}-\tilde{\boldsymbol{x}}_{k-N_{\text{MHE}}}\|_A^2 \\ &\quad+\Big\|\boldsymbol{d}-\tilde{\boldsymbol{d}}\Big\|_{A_d}^2+\sum_{i=k-N_{\text{MHE}}}^{k}\|\bar{\boldsymbol{y}}_i-\boldsymbol{y}(\boldsymbol{x}_i)\|_{Q_E}^2 \\ &\quad+\sum_{i=k-N_{\text{MHE}}}^{k-1}\|\boldsymbol{u}_i-\bar{\boldsymbol{u}}_i\|_{R_E}^2+\sum_{n=1}^{n_{\text{cbf}}}L_n(\boldsymbol{d}^n) &\text{(29a)}\\ &\text{s.t.}\quad \boldsymbol{x}_{i+1}=\boldsymbol{f}_d(\boldsymbol{x}_i)+g_d(x_i)\boldsymbol{u}_i, &\text{(29b)}\\ &(\nabla h_a^n(\boldsymbol{x}_i))^\top\Big(\boldsymbol{f}(\boldsymbol{x}_i)+\bar{\boldsymbol{w}}_f+ &\text{(29c)}\\ &\quad(g(\boldsymbol{x}_i)+w_g)\boldsymbol{u}_i\Big)+(\boldsymbol{H}^n(\boldsymbol{x}_i)-\boldsymbol{e}_h^n(\boldsymbol{x}_i))^\top\boldsymbol{\alpha} \\ &\quad\geq\|\boldsymbol{f}(\boldsymbol{x}_i)+\bar{\boldsymbol{w}}_f+(g(\boldsymbol{x}_i)+w_g)\boldsymbol{u}_i\|\,e_{\nabla h}^n(\boldsymbol{x}_i), \\ &\quad e_{\nabla h}^n(\boldsymbol{x}_i),e_h^n(\boldsymbol{x}_i)\geq 0,\quad n=1,\ldots,n_{\text{cbf}} &\text{(29d)}\end{aligned}$$

where the dynamics $\boldsymbol{f}_d$ and g_d respectively denote the discrete-time version of $\boldsymbol{f}$ and g, which are discretized using the fourth-order Runge-Kutta (RK4) method. In the MHE cost function (29a), the first two terms are the arrival costs weighted with matrices A,A_d, which aim at approximating the information prior to $k-N_{\text{MHE}}$, where $\tilde{\boldsymbol{x}},\tilde{\boldsymbol{d}}$ are the available estimations at time $k-N_{\text{MHE}}$. The measurements available at the time instant k are $\bar{\boldsymbol{u}}_i,\bar{\boldsymbol{y}}_i$ while their corresponding values obtained from the MHE model are $\boldsymbol{u}_i$ and $\boldsymbol{y}(\boldsymbol{x}_i)$, respectively. The cost terms $L_n,n=1,\ldots,n_{\text{cbf}}$ are selected as quadratic functions, e.g., $L_n(\boldsymbol{d}^n)=\boldsymbol{W}^\top\boldsymbol{d}^n\boldsymbol{W}$ with sufficiently large weights $\boldsymbol{W}$ in order to capture an accurate magnitude of the estimated truncation errors/disturbances in the proposed MHE-bsed RCBF. The estimated parameters and states at the time instant k are then used in the MPC scheme formulated

as

$$\min_{\boldsymbol{x},\boldsymbol{u},\boldsymbol{\sigma}} \quad V^f(\boldsymbol{x}_{k+N_{\text{MPC}}}) + \Gamma_{k+N_{\text{MPC}}}(\boldsymbol{\sigma}_{k+N_{\text{MPC}}}) + \sum_{i=k}^{k+N_{\text{MPC}}-1} l(\boldsymbol{x}_i, \boldsymbol{u}_i) + \Gamma_i(\boldsymbol{\sigma}_i) \tag{30a}$$

$$\text{s.t.} \quad \boldsymbol{x}_{i+1} = \boldsymbol{f}_d(\boldsymbol{x}_i) + g_d(x_i)\,\boldsymbol{u}_i, \tag{30b}$$

$$\boldsymbol{x}_k = \hat{\boldsymbol{x}}_k, \quad \boldsymbol{d}^n = \hat{\boldsymbol{d}}_k^n \tag{30c}$$

$$\boldsymbol{I}(\boldsymbol{u}_i) \leq 0, \tag{30d}$$

$$\boldsymbol{P}(\boldsymbol{x}_i, \boldsymbol{u}_i) \leq \boldsymbol{\sigma}_i, \quad \boldsymbol{P}^f(\boldsymbol{x}_{k+N_{\text{MPC}}}) \leq \boldsymbol{\sigma}_{k+N_{\text{MPC}}}, \tag{30e}$$

$$\boldsymbol{\sigma}_{k,\ldots,k+N_{\text{MPC}}} \geq 0, \tag{30f}$$

$$\begin{aligned}(\nabla h_a^n(\boldsymbol{x}_i))^\top \Big(\boldsymbol{f}(\boldsymbol{x}_i) + \bar{\boldsymbol{w}}_f + \\ (g(\boldsymbol{x}_i) + w_g)\,\boldsymbol{u}_i\Big) + (\boldsymbol{H}^n(\boldsymbol{x}_i) - \boldsymbol{e}_h^n(\hat{\boldsymbol{x}}_k))^\top \boldsymbol{\alpha} \\ \geq \|\boldsymbol{f}(\boldsymbol{x}_i) + \bar{\boldsymbol{w}}_f + (g(\boldsymbol{x}_i) + w_g)\,\boldsymbol{u}_i\|\, e_{\nabla h}^n(\hat{\boldsymbol{x}}_k), \\ n = 1, \ldots, n_{\text{cbf}}\end{aligned} \tag{30g}$$

where V^f, l are the terminal and the stage cost functions, respectively. $\boldsymbol{I}$ collects the input inequality constraints while $\boldsymbol{P}^f$ and $\boldsymbol{P}$ are the mixed terminal and stage inequality constraints. To guarantee feasibility of the MPC scheme above, we relax the constraints by introducing the slack variables $\boldsymbol{\sigma}_i$, which are penalized by using a function of the form $\Gamma_i(\boldsymbol{\sigma}_i) = \boldsymbol{w}^\top \boldsymbol{\sigma}_i$ with sufficiently large weights $\boldsymbol{w}$.

VI. Simulation Results and Discussion

In this section, we examine the performance of the proposed MHE-based approximate RCBF-MPC for AUVs motion planning. In this scenario, an AUV aims at arriving a final destination B from an initial position A while safely navigating around unsafe zones in the presence of external disturbances. To model the external disturbances $\boldsymbol{d} = M^{-1}(\boldsymbol{x}_1)\boldsymbol{p}$, the perturbation terms $\boldsymbol{p} = [p_1, p_2, p_3, p_4]^\top$ are selected as

$$\begin{aligned}&p_1 = p_2 = 20\sin(0.08t), \quad p_3 = 10\sin(0.08t), \\ &p_4 = \mathcal{N}(0, \sigma^2), \sigma = 0.1.\end{aligned} \tag{31}$$

The continuous-time dynamics is discretized using an RK4 with a sampling time of 0.05 sec. Both the prediction and estimation horizons are set to $N_{\text{MPC}} = N_{\text{MHE}} = 8$. In the parametric CBF setting, we only consider two odd-powered safety functions as $\boldsymbol{H}(\boldsymbol{x}_k) = \left[h_a(\boldsymbol{x}_k), (h_a(\boldsymbol{x}_k))^3\right]^\top$, and select $\boldsymbol{\alpha} = [1, 1]^\top$. Each safety function h_a is described by a sphere equation dedicated to each unsafe zone. The constraints on the control inputs and states are as

$$\begin{aligned}&-20 \leq \tau_1 \leq 20, \quad -15 \leq \tau_2 \leq 15, \quad -1 \leq \tau_4 \leq 1 \\ &-0.2 \leq u, v, w \leq 0.2.\end{aligned} \tag{32}$$

The AUV model parameters are selected the same as those in [13]. As observed in Fig. 1, the magenta path generated by the MPC-CBF intersects the obstacle 1 as the CBF scheme is not robust against the truncation errors/disturbances. To compare the performance of the proposed MHE-based approximate RCBF with the existing discrete-time CBF, we show the blue, purple and black paths generated by the MPC-CBF when the CBF scheme is formulated as (17) with $\gamma = 0.01$ and $\gamma = 0.05$ and $\gamma = 0.1$, respectively. Although we select the three constants γ small enough to provide the maximum safety (more conservative), this approach still fails to ensure a collision-free navigation as the corresponding paths cannot safely pass the unsafe zones represented by obstacles $1, 2, 4$. More specifically, the external disturbances cause a model mismatch so that the model used in the MPC scheme cannot capture the true dynamics of AUV, and consequently the discrete-time CBFs are no longer able to tackle the effects of this model mismatch. The cyan line shows the path generated by the proposed MPC scheme combined with an MHE-based approximate RCBF. This approach provides a collision-free navigation as the CBF scheme is robust against both the truncation errors and external disturbances captured by the MHE scheme (29). The evolution of adaptive parameters of

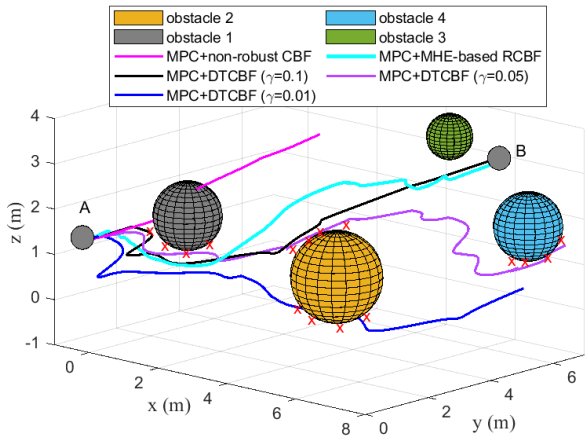

Fig. 1. The magenta line shows the path planning result when the CBFs are non-parametric, and the truncation errors/disturbances are not considered in the CBF condition. The blue, purple and black lines illustrate the paths generated using the non-parametric CBFs, where the discrete-time CBF condition (17) is used. The cyan line shows the path generated using the proposed MHE-based approximate RCBF with parametric CBFs, where the mapping function is constructed by the odd-powered functions (28). The red crosses show the locations where collisions occur.

the proposed approximate RCBF is shown in figures 2 and 3. The constrained control inputs are shown in Fig. 4. As shown in Fig. 3, the three CBFs representing the obstacles $1, 2, 4$ are heavily affected by the external disturbances as the estimations of the augmented perturbations have some high frequency fluctuations, a.k.a chattering when AUV is passing the areas around these unsafe zones (obstacles $1, 2, 4$). The proposed MHE-based RCBF then enhances the performance of CBFs by estimating these augmented perturbations such that the CBF models used in the MPC scheme can adaptively adjust their structure and capture a more accurate model of the real environment.

VII. Conclusion

In this paper, a safe motion planning approach for AUVs has been proposed, where we formulated a robust discrete-time CBF in an MPC scheme to address the safety problem in

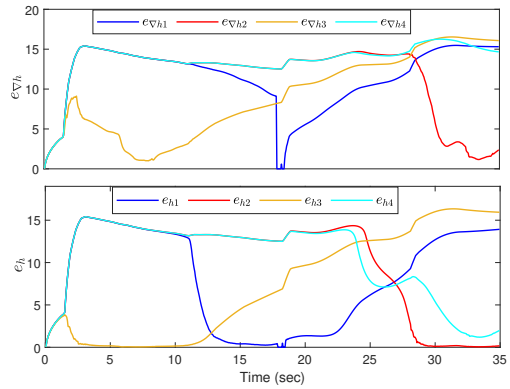

Fig. 2. Evolution of the estimated bounds $e_h, e_{\nabla h}$ using the proposed MHE-based approximate robust CBF.

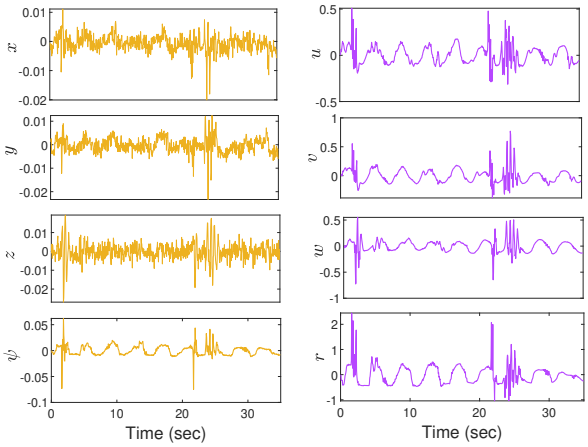

Fig. 3. Estimation of the augmented perturbations (truncation errors/disturbances) $\bar{w}_f$ added to the system states $\boldsymbol{\eta}$ and $\dot{\boldsymbol{\eta}}$ using the proposed MHE-based approximate robust CBF.

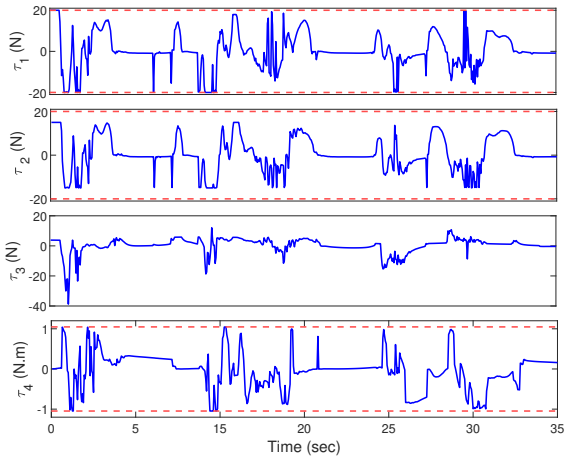

Fig. 4. Evolution of the control inputs using the proposed MHE-based approximate robust CBF.

the presence of external disturbances. The proposed discrete-time CBF has the same structure as the continuous-time CBFs, which allows us to construct a robust CBF in order to cope with unknown CBFs and external disturbances. To capture both the external disturbances and the truncation errors due to discretization of the continuous-time CBFs, and estimate several parameters required in the proposed CBF-MPC scheme, we then proposed to use an MHE scheme to construct an approximate robust CBF. Simulation results demonstrated the advantages our proposed safe control approach provided compared to several other methods for path planning of AUVs.

REFERENCES

[1] J. Dowdeswell, J. Evans, R. Mugford, G. Griffiths, S. McPhail, N. Millard, P. Stevenson, M. Brandon, C. Banks, K. Heywood, and et al., "Autonomous underwater vehicles (AUVs) and investigations of the ice–ocean interface in antarctic and arctic waters," *Journal of Glaciology*, vol. 54, no. 187, p. 661–672, 2008.

[2] J. B. Rawlings, D. Q. Mayne, and M. Diehl, *Model predictive control: theory, computation, and design*. Nob Hill Publishing Madison, WI, 2017, vol. 2.

[3] J. Zeng, B. Zhang, and K. Sreenath, "Safety-critical model predictive control with discrete-time control barrier function," in *2021 American Control Conference (ACC)*. IEEE, 2021, pp. 3882–3889.

[4] H. Nejatbakhsh Esfahani, S. Ahmadi, and J. Mohammadpour Velni, "Learning-based safety critical model predictive control using stochastic control barrier functions," in *2024 American Control Conference (ACC)*. IEEE, 2024.

[5] A. D. Ames, X. Xu, J. W. Grizzle, and P. Tabuada, "Control barrier function based quadratic programs for safety critical systems," *IEEE Transactions on Automatic Control*, vol. 62, no. 8, pp. 3861–3876, 2017.

[6] A. D. Ames, S. Coogan, M. Egerstedt, G. Notomista, K. Sreenath, and P. Tabuada, "Control barrier functions: Theory and applications," in *2019 18th European control conference (ECC)*. IEEE, 2019, pp. 3420–3431.

[7] A. Forsgren, P. E. Gill, and M. H. Wright, "Interior methods for nonlinear optimization," *SIAM review*, vol. 44, no. 4, pp. 525–597, 2002.

[8] N. N. Minh, S. McIlvanna, Y. Sun, Y. Jin, and M. Van, "Safety-critical model predictive control with control barrier function for dynamic obstacle avoidance," *arXiv preprint arXiv:2211.11348*, 2022.

[9] R. Tallamraju, S. Rajappa, M. J. Black, K. Karlapalem, and A. Ahmad, "Decentralized mpc based obstacle avoidance for multi-robot target tracking scenarios," in *2018 IEEE International Symposium on Safety, Security, and Rescue Robotics (SSRR)*. IEEE, 2018, pp. 1–8.

[10] K. Garg and D. Panagou, "Robust control barrier and control Lyapunov functions with fixed-time convergence guarantees," in *2021 American Control Conference (ACC)*, 2021, pp. 2292–2297.

[11] E. Daş, S. X. Wei, and J. W. Burdick, "Robust control barrier functions with uncertainty estimation," 2023.

[12] H. Nejatbakhsh Esfahani, A. Bahari Kordabad, W. Cai, and S. Gros, "Learning-based state estimation and control using mhe and mpc schemes with imperfect models," *European Journal of Control*, vol. 73, p. 100880, 2023. [Online]. Available: https://www.sciencedirect.com/science/article/pii/S0947358023001085

[13] H. N. Esfahani, B. Aminian, E. I. Grøtli, and S. Gros, "Backstepping-based integral sliding mode control with time delay estimation for autonomous underwater vehicles," in *2021 20th International Conference on Advanced Robotics (ICAR)*, 2021, pp. 682–687.

[14] W. Shaw Cortez, D. Oetomo, C. Manzie, and P. Choong, "Control barrier functions for mechanical systems: Theory and application to robotic grasping," *IEEE Transactions on Control Systems Technology*, vol. 29, no. 2, pp. 530–545, 2021.

[15] J. Schilliger, T. Lew, S. M. Richards, S. Hänggi, M. Pavone, and C. Onder, "Control barrier functions for cyber-physical systems and applications to NMPC," *IEEE Robotics and Automation Letters*, vol. 6, no. 4, pp. 8623–8630, 2021.

[16] L. Wang, A. D. Ames, and M. Egerstedt, "Safety barrier certificates for collisions-free multirobot systems," *IEEE Transactions on Robotics*, vol. 33, no. 3, pp. 661–674, 2017.